Molecular Crystals and Liquid Crystals
Publication details, including instructions for authors and subscription information:
http://www.tandfonline.com/loi/gmcl20

Electronic Structure of Polymeric μ-Cyclopentadienyl Transition Metal Atom Complex

Y. Matsuura [a]

[a] Nara National College of Technology, Yamato-koriyama, Nara, Japan

Version of record first published: 07 Oct 2011

To cite this article: Y. Matsuura (2011): Electronic Structure of Polymeric μ-Cyclopentadienyl Transition Metal Atom Complex, Molecular Crystals and Liquid Crystals, 548:1, 265-271

To link to this article: http://dx.doi.org/10.1080/15421406.2011.556537

Mol. Cryst. Liq. Cryst., Vol. 548: pp. 265–271, 2011

ISSN: 1542-1406 print/1563-5287 online
DOI: 10.1080/15421406.2011.556537

Taylor & Francis
Taylor & Francis Group

Electronic Structure of Polymeric μ-Cyclopentadienyl Transition Metal Atom Complex

Y. MATSUURA*

Nara National College of Technology, Yamato-koriyama, Nara, Japan

We focused on cyclopentadienyl ring–metal atom [(Cp)—M (M = Fe, Co, Ni)] complexes adsorbed on an Au or Pt slab and examined the electronic structure by performing tight-binding band calculations. The calculation results suggested a change in the bonding character of the C—M bond in the complex adsorbed on the Pt slab. It was found that the Cp—Ni complex was energetically feasible with regard to its adsorption on the Pt slab. On the other hand, other Cp—M (M = Fe and Co) complex was not stabilized by the adsorption on the Au or Pt slab.

Keywords Aromatics; gold; interface states; platinum

1. Introduction

In recent times, nano/molecular electronic devices have been studied extensively because these devices can enhance circuit performance. In the future, it is expected that the two-terminal junction of molecules with metal electrodes will serve as building blocks for the fabrication of nano/molecular electronic devices [1]. Sandwich-type cyclopentadienyl ring–metal atom (Cp—M) complexes have been studied extensively for electronic materials [2]. The synthesis of a series of polymeric Cp—M complexes has been reported in the literature [3, 4]. Theoretical studies suggest that sandwich-type molecular wires of Cp–transition metal atoms could be applied to a molecular spin filter [5–7]. Especially, it was found that Cp—Ni complex sandwiched between two gold electrodes provided the remarkable spin-transport properties by changing the contact geometry [6].

Adsorption of hydrocarbon compounds on transition metal surfaces has been studied extensively to enable the conversion of aliphatic linear-chain hydrocarbons to aromatic and branched species [8]. It is well known that among these compounds, aromatic compounds such as benzene and cyclopentadienyl energetically prefer to be adsorbed on a Pt(111) surface [9]. Therefore, it is also assumed that the Cp ring at the edge of the Cp—M complexes can be stabilized on the Pt(111) surface of the metal electrode. We have studied the electronic structures of a Cp–indium complex adsorbed on a Pt slab and have clarified that the complex was energetically stabilized by the bonding character of the C–indium bond, which exhibited an anti-bonding character before the adsorption [10].

In this study, we focused on the future applications of Cp—M (M = Fe, Co, Ni) complexes to nano/molecular electronic devices because high-spin filter efficiency properties

*Address correspondence to Yukihito Matsuura, Nara National College of Technology, 22 Yata-cho, Yamato-koriyama, Nara 639-1080, Japan. Tel.: +81-743-55-6158; Fax: +81-743-55-6169. E-mail: matsuura@chem.nara-k.ac.jp

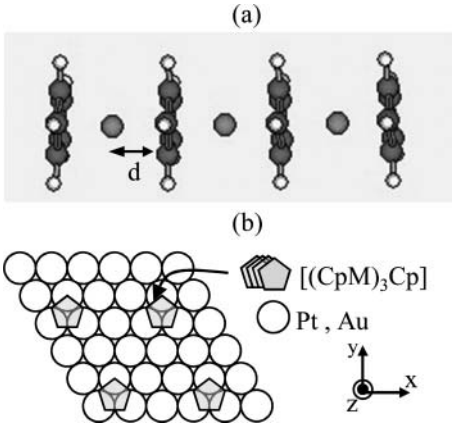

Figure 1. (a) Chemical structures of the Cp−M complex (M = V, Fe, Co, Ni). (b) Top view of the (3 × 3) Pt(111) or Au(111) surface, on which [$(CpM)_3Cp$] is absorbed.

have been prospected in the complexes [5–7]. It is important to consider the possibility of an interconnection between the complex and a metal electrode. To understand the interaction between the Cp−M complex and a Pt or Au electrode, we examined the 2D band structures of Cp−M complex adsorbed on a Pt or Au slab.

2. Calculation Method

Because it was possible to examine the electronic structures of both the edge part and the central region of the Cp−M complex, we constructed a model of Cp−M (M = Fe, Co, Ni) complex that consisted of three metal atoms and four Cp rings ([$(CpM)_3Cp$]). The structures of [$(CpM)_3Cp$] were obtained from the calculation results of polymeric Cp−M complexes [6], whose structures had a linear, eclipsed form with D_{5h} symmetry, as shown in Fig. 1(a). The Cp−M distances of the complexes are summarized in Table 1.

In the model of a Cp−M complex adsorbed on a Pt slab, the Pt–Pt bond length was determined to be 2.77 Å. Figure 1(b) shows the Pt slab formed by the deposition of four Pt layers along the Z-axis. [$(CpM)_3Cp$] is aligned on the Pt slab in the XY plane, as shown in Fig. 1(b); this alignment is the same as that in Sung and Hoffmann [11]. The arrangement of [$(CpM)_3Cp$] on the Pt slab is described using a model of Cp^- on a Pt(111) surface designed by Hoffmann [12]. In order to optimize the structures of [$(CpM)_3Cp$] on the Pt slab, the distance of the Cp−Pt surface was varied from 1.8 Å to 5.0 Å. In this optimization process, the structures of [$(CpM)_3Cp$] and the Pt slab were kept as the first constructed models. We also performed the band calculation for [$(CpM)_nCp$] (n = 2, 4, 5) adsorbed on the Pt slab.

Table 1. Distances (d) of [$(CpM)_3Cp$] (M = Fe, Co, and Ni)

	Fe	Co	Ni
d (Å)	3.41	3.50	3.68

Table 2. Parameters for atoms

Atom	Orbital	H_{ii} (eV)	ζ_1	ζ_2	C_1	C_2
H	1s	−13.6000	1.3000			
C	2s	−21.4000	1.6250			
	2p	−11.4000	1.6250			
Fe	4s	−9.1000	1.9000			
	4p	−5.3200	1.9000			
	3d	−12.6000	5.3500	2.0000	0.5505	0.6260
Co	4s	−9.2100	2.0000			
	4p	−5.2900	2.0000			
	3d	−13.1800	5.5500	2.1000	0.5679	0.6059
Ni	4s	−10.9500	2.1000			
	4p	−6.2700	2.1000			
	3d	−14.2000	5.7500	2.3000	0.5493	0.6082
Au	6s	−10.9200	2.6020			
	6p	−5.5500	2.5840			
	5d	−15.0700	6.1630	2.7940	0.6442	0.5356
Pt	6s	−9.0770	2.5540			
	6p	−5.4750	2.5540			
	5d	−12.5900	6.0130	2.6960	0.6334	0.5513

Furthermore, we have constructed a model of an Au slab similar to that of the Pt slab and have calculated its band structures. The Au–Au bond length was determined to be 2.86 Å.

Subsequently, we calculated the 2D band structure of a model in which $[(CpM)_3Cp]$ was adsorbed on a Pt(111) surface by using the extended Hückel approximation [13]. Although the extended Hückel approximation is a qualitative method, it is well known that this method is suitable for analyzing the bonding character by using the overlap population. The band calculations were performed using the YAeHMOP program [14]. The atomic parameters (H_{ii} = orbital energy, ζ = Slater exponent) listed in Table 2 were used for the calculation. Slater exponent ζ determined the Slater-type orbitals of the atomic orbitals for the extended Hückel approximation as follows:

$$\Phi_{\mathrm{nlm}}(r, \theta, \phi) = N r^{n-1} \exp(-\zeta r) Y_{\mathrm{lm}}(\theta, \phi).$$

In a modified Wolfsberg–Helmholz formula, the off-diagonal matrix elements H_{ij} can be evaluated as follows:

$$\begin{aligned} H_{ij} &= 1/2 K S_{ij}(H_{ii} + H_{jj}), \\ K &= k + \Delta^2 + \Delta^4(1 - k); k = 1.75, \\ \Delta &= (H_{ii} - H_{jj})/(H_{ii} + H_{jj}), \end{aligned}$$

where i and j are the atomic orbitals, and S_{ij} is the overlap matrix between the Slater-type orbitals of the atomic orbitals. In this band calculation, 20 representative wave vectors (k) were selected from 0 to π/a (a is the unit cell length) at regular intervals.

3. Results and Discussion

3.1 [(CpNi)$_3$Cp] on the Pt or Au Slab

As shown in Fig. 2, the distance of the Cp—M (M = Au and Pt) surface was varied from 1.8 Å to 5.0 Å. The total energy of a unit cell in [(CpNi)$_3$Cp] on the Pt slab reached its minimum value at 2.4 Å, as shown in Fig. 2(a). On the other hand, Fig. 2(b) shows that the total energy of that on the Au slab decreased with increasing the Cp–Au distance. Therefore, the energetic stabilization of [(CpNi)$_3$Cp] allowed adsorption on the Pt slab to occur at this minimum value.

In order to examine the origin of stabilization at this value, we examined the frontier orbitals of [(CpNi)$_3$Cp], as shown in Figs. 3(a) and (b). [(CpNi)$_3$Cp] had a closed-shell system consisting of 130 electrons. The energy levels of the highest occupied molecular orbital (HOMO) (Orbitals 64 and 65) and the lowest unoccupied molecular orbital (LUMO) (Orbitals 66 and 67) were located at −11.05 and −10.52 eV, respectively. The HOMO degenerated and exhibited an anti-bonding character between the Ni $3d_{xz}$ and Cp e_1 orbitals. Furthermore, the next HOMO (HOMO – 1) exhibited a slightly anti-bonding character between the Ni $3d_{xz}$ and Cp e_1 orbitals at the edge of [(CpNi)$_3$Cp]. Additionally, we have calculated the density of state (DOS) of the Pt slab and the Au slab from their band structures, as shown in Figs 3(c) and (d). The Fermi level of the Pt slab is located at an energy level of −11.21 eV and that of the Au slab at −9.68 eV. In the band structure of the Pt slab, the electrons at the energy levels near the Fermi level are mainly assigned to 3d orbitals. In the case of the Au slab, however, those electrons belong to 4s orbitals.

To analyze the interaction between [(CpNi)$_3$Cp] and the Pt slab, we examined the band structures and the frontier orbitals of [(CpNi)$_3$Cp] on the Pt slab whose Cp—Pt distance was 2.4 Å. The energy levels of the HOMO of [(CpNi)$_3$Cp] were located at the energy levels

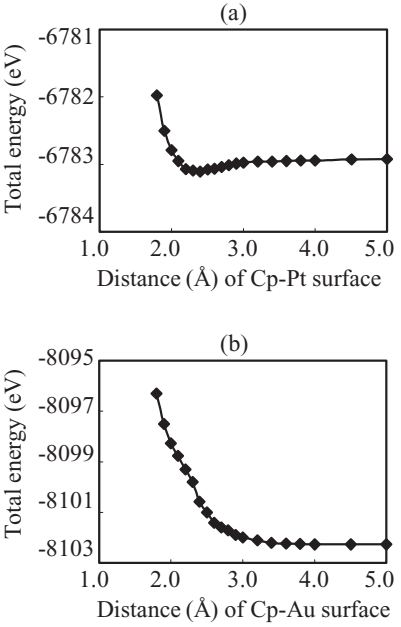

Figure 2. Total energy of (a) [(CpNi)$_3$Cp] on Pt stab and (b) [(CpNi)$_3$Cp] on Au stab.

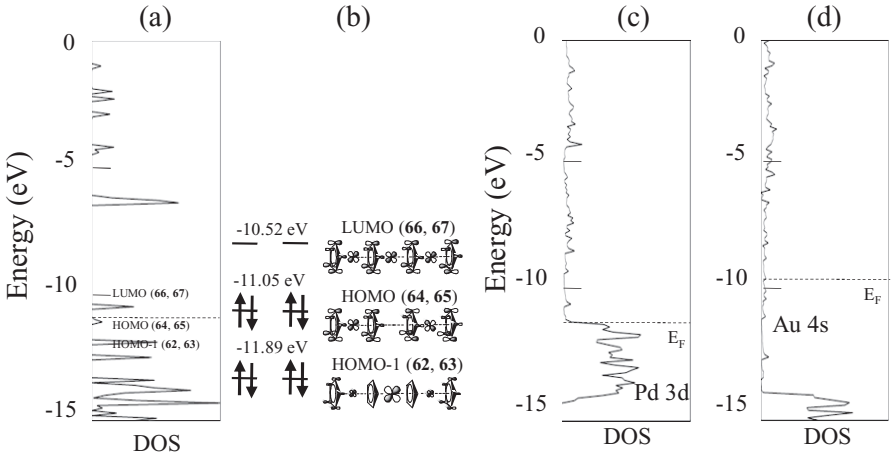

Figure 3. (a) DOS and (b) frontier orbitals of $[(CpNi)_3Cp]$. DOS of (c) Pt slab and (d) Au slab.

above the Fermi level (−11.21 eV) of the Pt slab. Therefore, the adsorption of $[(CpNi)_3Cp]$ resulted in the interaction of these electrons to the Pt slab. As a result, as shown in Fig. 4(a), the Fermi level of $[(CpNi)_3Cp]$ on the Pt slab was lower than the Fermi level of $[(CpNi)_3Cp]$ (Fig. 3(c)). We also examined the projected DOS (PDOS) for Ni atom, as shown in Fig. 4(b). The PDOS for Ni atoms at the energy that corresponded to Orbitals 64 and 65 in $[(CpNi)_3Cp]$ (Fig. 3(b)) became vacant in $[(CpNi)_3Cp]$ on the Pt slab (Fig. 4(b)) Therefore, the donation of electrons of HOMO (Orbitals 64 and 65) occurred by the adsorption on the Pt slab. Weakening the anti-bonding character of the Cp—Ni bond by the adsorption on the Pt slab provided the energetic stabilization.

On the other hand, although it was not an energetically stable point, we examined the interaction between $[(CpNi)_3Cp]$ and the Au slab whose Cp—Au distance was 2.4 Å. The energy levels of the HOMO of $[(CpNi)_3Cp]$ is lower than that of the Fermi level (−9.68 eV)

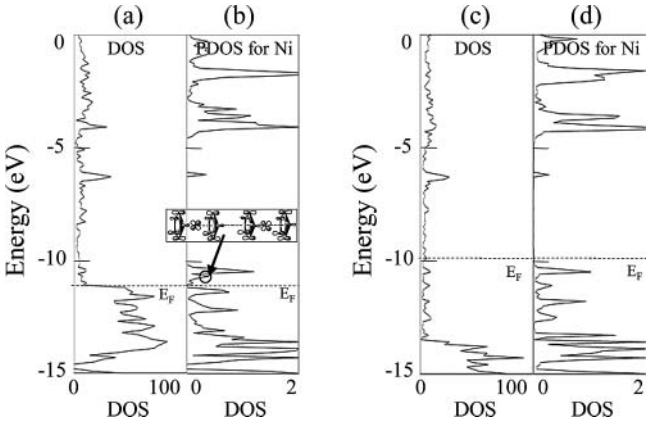

Figure 4. (a) DOS and (b) PDOS for Ni atom of $[(CpNi)_3Cp]$ on Pt slab. (c) DOS and (d) PDOS for Ni atom of $[(CpNi)_3Cp]$ on Au slab. The MO pattern in (b) shows a part of the MO pattern of $[(CpNi)_3Cp]$ adsorbed on the Pt slab.

of the Au slab. Therefore, after the adsorption of $[(CpNi)_3Cp]$ on the Au slab, the energy levels of the LUMO of $[(CpNi)_3Cp]$ are filled by the electrons derived from the Au slab, which is confirmed in Fig. 4(d). The HOMO of $[(CpNi)_3Cp]$ on the Au slab exhibited anti-bonding character of Cp—Ni bond with a resultant of unstabilization of $[(CpNi)_3Cp]$. Therefore, there is no minimum point of the total energy of $[(CpNi)_3Cp]$ on the Au slab when varying a Cp—Au distance.

Finally, we also performed the band calculation for $[(CpNi)_nCp]$ ($n = 2, 4, 5$) adsorbed on the Pt slab. Although the details have not been mentioned here, the change in the total energy exhibited the same tendency as that when the distance of the Cp—Pt surface was varied in $[(CpNi)_3Cp]$ on the Pt slab. The stabilization of $[(CpNi)_nCp]$ on the Pt slab is not dependent on the size of $[(CpNi)_nCp]$.

3.2 [(CpM)$_3$Cp] (M = Co and Fe) on the Pt Slab

Subsequently, we examined the dependence of the change in the total energy of $[(CpCo)_3Cp]$ adsorbed on the Pt slab dependent on the distance of the Cp—Pt surface. The obtained plot suggests that no stable point exists in the adsorption system of $[(CpCo)_3Cp]$ on the Pt slab. We also examined the frontier orbitals of the complex. It has 127 electrons, which is fewer electrons than in $[(CpNi)_3Cp]$. Therefore, in the case of $[(CpCo)_3Cp]$, the degenerated Orbitals 64 and 65, which are the same as shown in Fig. 3(b), possess one electron to form the singly occupied molecular orbital (SOMO). The SOMO is located at an energy level of -10.69 eV, which is higher than the Fermi level (-11.21 eV) of the Pt slab. Although the SOMO exhibits an anti-bonding character, it appears that the interaction of only one electron from Orbital 64 or 65 to the Pt slab does not efficiently allow the stable adsorption of $[(CpCo)_3Cp]$ on the Pt slab.

The same conclusion can be drawn in the case of $[(CpFe)_3Cp]$. A plot of the total energy against the distance of the Cp—Pt surface suggests the presence of an unstable energetic state of $[(CpFe)_3Cp]$ on the Pt slab. Because $[(CpFe)_3Cp]$ has 124 electrons, it has two SOMOs at the energy level of -10.14 eV, which are the same as Orbitals 62 and 63, shown in Fig. 3(b). The slightly anti-bonding character of Cp—Fe in the SOMOs is also incapable of providing an efficiently energetic stabilization for the adsorption of $[(CpFe)_3Cp]$ on the Pt slab.

4. Conclusion

In summary, the electronic structure of Cp—M complex adsorbed on an Au or Pt slab was examined by performing tight-binding band calculations. The calculation result suggests that the Cp—Ni complex was energetically stabilized on the Pt slab. The donation of electrons whose frontier orbitals exhibit an anti-bonding character results in the stabilization of the Cp—Ni complex adsorbed on the Pt slab. From these results, the Cp—Ni complexes adsorbed on the Pt slab are expected to be applicable to a molecular spin filter for the future spintronic devices [15].

Acknowledgment

The author would like to thank Prof. R. Hoffmann and his coworkers for permission to use the YAeHMOP program.

References

[1] Qian, Z., Li, R., Hou, S., Xue, Z., & Sanvito, S. (2007). *J. Chem. Phys.*, *127*, 194710.
[2] Barlow, S., & O'Hare, D. (1997). *Chem. Rev.*, *97*, 637.
[3] Jutzi, P., & Burford, N. (1999). *Chem. Rev.*, *99*, 969.
[4] Nagao, S., Kato, A., Nakajima, A., & Kaya, K. (2000). *J. Am. Chem. Soc.*, *122*, 4221.
[5] Zhou, L., Yang, S. W., Ng, M. F., Sullivan, M. B., Tang, B. B. C., & Shen, L. (2008). *J. Am. Chem. Soc.*, *130*, 4023.
[6] Yi, Z., Shen, X., Sun, L., Shen, Z., Hou, S., & Sanvito, S. (2010). *ACS Nano*, *4*, 2274.
[7] Shen, X., Yi, Z., Shen, Z., Zhao, X., Wu, J., Hou, S., & Sanvito, S. (2009). *Nanotechnology*, *20*, 385401.
[8] Kang, D., & Anderson, A. (1985). *J. Am. Chem. Soc.*, *107*, 7858.
[9] Brizuela, G., & Castellani, N. J. (1998). *Surf. Sci.*, *401*, 297.
[10] Matsuura, Y., & Uchimiya, R. (2010). *Solid State Commun.*, *150*, 1400.
[11] Sung, S., & Hoffmann, R. (1985). *J. Am. Chem. Soc.*, *107*, 578.
[12] Brizuela, G., & Hoffmann, R. (1998). *J. Phys. Chem. A*, *102*, 9618.
[13] Hoffmann, R. (1963). *J. Chem. Phys.*, *39*, 1397.
[14] Landrum, G. A. (1997). *Yet Another Extended Hückel Molecular Orbital Package (YAeHMOP)*, Cornell University: Ithaca, NY.
[15] Shen, L., Yang, S., Ng, M., Ligatchev, V., Zhou, L., & Feng, Y. (2008). *J. Am. Chem. Soc.*, *130*, 13956.